Level structure of ^{18}Ne and its importance in the ^{14}O(α,p)^{17}F reaction rate

S. Almaraz-Calderon, W. P. Tan, A. Aprahamian, B. Bucher, A. Roberts, M. Wiescher, C. R. Brune, T. N. Massey, N. Özkan, R. T. Güray, and H. Mach

THE LEVEL STRUCTURE OF ^{18}Ne AND ITS IMPORTANCE IN THE ^{14}O(α,p)^{17}F REACTION RATE.

S. Almaraz-Calderon,[*] W. P. Tan,[†] A. Aprahamian, B. Bucher, A. Roberts, and M. Wiescher

Nuclear Science Laboratory, University of Notre Dame, Notre Dame, IN 46556, USA

C. R. Brune and T. N. Massey

Department of Physics and Astronomy, Ohio University, Athens, OH 45701, USA

N. Özkan[‡] and R. T. Güray[‡]

Department of Physics, Kocaeli University, 41380 Kocaeli, Turkey

H. Mach[‡]

Department of Radiation Sciences, ISV, Uppsala University, Uppsala, Sweden

The level structure of ^{18}Ne above the α-decay threshold has been studied using the ^{16}O(^{3}He,n) reaction. A coincidence measurement of neutrons and charged particles decaying from populated states in ^{18}Ne has been made. Decay branching ratios were measured for six resonances and used to calculate the ^{14}O(α,p)^{17}F reaction rate which is a measure of one of two breakout paths from the Hot CNO cycle. The new experimental information combined with previous experimental and theoretical information provides a more accurate calculation of the reaction rate.

PACS numbers: 26.30.-k, 23.20.Lv, 25.55.-e, 26.30.-k, 98.70.Qy

[*] salmaraz@nd.edu; Present Address: Physics Division, Argonne National Laboratory, Argonne, IL 60439

[†] wtan@nd.edu

[‡] Nuclear Science Laboratory, University of Notre Dame, Notre Dame, IN 46556, USA

I. INTRODUCTION

The level structure of ^{18}Ne above the charged particle decay threshold plays a fundamental role in one of two possible break-out paths from the Hot Carbon-Nitrogen-Oxygen (HCNO) cycle. In explosive astrophysical scenarios such as novae and X-ray bursts, when temperatures are $T_9 \geq 0.1$, it is possible to bypass the β-decay of the waiting points in the HCNO cycle, such as the nuclei ^{14}O and ^{15}O, by α capture reactions leading directly to the αp-process and the rp-process [1]. The two breakout paths from the HCNO cycle are the reaction sequences ^{14}O$(\alpha,$p$)^{17}$F$($p$,\gamma)^{18}$Ne$(\alpha,$p$)$ and ^{15}O$(\alpha,\gamma)^{19}$Ne$($p$,\gamma)$ shown in Fig. 1, labeled as Breakout I and Breakout II respectively and indicated in red arrows.

In breakout path I, the ^{14}O$(\alpha,$p$)^{17}$F$($p$,\gamma)^{18}$Ne reaction chain proceeds through resonance states in ^{18}Ne. These breakout reaction rates are very sensitive to the spins, energies, and the partial/total widths of the relevant resonances in ^{18}Ne. In fact, the direct reaction contribution to the ^{14}O$(\alpha,$p$)^{17}$F rate has been shown to be very small at relevant astrophysical temperatures in comparison to the resonance contributions [1].

The states that contribute to the ^{14}O$(\alpha,$p$)^{17}$F reaction rate are the ones above the α-decay threshold ($E_x \geq 5.1246$ MeV) in ^{18}Ne as shown in the level scheme of ^{18}Ne in Fig. 2. Reliable experimental information on these levels, despite various efforts in the past, is still largely missing, in part due to the radioactive nature of this nucleus and the complicated decay scheme of resonances. The properties of these levels and their contribution to the ^{14}O$(\alpha,$p$)^{17}$F reaction rate were first reported by Wiescher $et\ al.$ [1] where the widths and spin assignments of the relevant levels in ^{18}Ne were estimated from the properties of the mirror nucleus ^{18}O. Hahn $et\ al.$ [2] used a series of indirect measurements to study the ^{14}O$(\alpha,$p$)^{17}$F rate by populating and detecting the relevant levels in ^{18}Ne. However, the measurements on the indirect reactions did not yield any information on partial widths. Other studies, measured the time-reversed reaction using a ^{17}F radioactive beam by groups at ANL [4] and ORNL [5], however the contribution via the first excited state in ^{17}F, in particular for the 6.15 MeV state yielded conflicting results [6–8]. There was also an attempt at a direct measurement at RIKEN using radioactive ^{14}O beam and a helium target [9]. There are however serious discrepancies between the direct and time-reversed measurements including a large contribution from the 7.06 MeV state decaying to the first excited state in ^{17}F that was reported in the direct measurement to increase the rate by 50 % [9]. In order to resolve these discrepancies we measured resonance levels in ^{18}Ne and their decay branching ratios by the ^{16}O$(^3$He,n$)$ reaction.

For all the levels above the α-decay threshold in ^{18}Ne, only natural-parity states contribute to the ^{14}O$(\alpha,$p$)^{17}$F reaction rate since in the ^{14}O $+ \alpha$ entrance channel both nuclei have ground state spins of 0^+. In addition to the α-decay, several other particle decay channels are also open: p-channel to the ground state of ^{17}F (Q $= 3.934$ MeV), p'-channel to the first excited state ($E_x = 0.4953$ MeV) of ^{17}F (Q $= 4.429$ MeV), $2p$-channel to the ground state of ^{16}O (Q $= 4.534$ MeV) and α-channel to the ground state of ^{14}O (Q $= 5.125$ MeV) as shown in Fig. 2. These partial branching ratios may need to be taken into account when calculating the reaction rate.

Information on the α-widths, in particular for the 6.15 MeV state, is critical for calculating the reaction rate since the proton decay channels dominate [1]. However, no direct measurements of the α-decay branching ratios have been made for these levels. Using the indirect Asymptotic Normalization Coefficient (ANC) approach, the FSU group estimated the α-width of the most important 1^- state at 6.15 MeV based on their work on the mirror level in ^{18}O [10].

Furthermore, determination of the ratio of the partial widths $\Gamma_{p'}/\Gamma_p$ has a strong relevance in order to extract the reaction rate from the measurement of the inverse reaction ^{17}F$($p$,\alpha)^{14}$O where only the p channel can be measured and a correction is required using the $\Gamma_{p'}/\Gamma_p$ branching. As mentioned above, the p'-decay channel has been reported for the 6.15 MeV level [7, 8] and the 7.06 MeV level [9]. But the disagreements between existing results [6–8] left the partial widths still largely unconstrained. On the other hand, measurement of the Γ_{2p} is important if it is large enough because it can effectively reduce the resonance strength. Gomez del Campo $et\ al.$ [11] reported evidence of two-proton decay from the $E_x = 6.15$ MeV level.

In the present work, the chosen reaction favors the natural-parity states in ^{18}Ne that are expected to contribute to the ^{14}O$(\alpha,$p$)^{17}$F reaction rate. We measured the coincidences between neutrons and charged particles in order to allow the determination of the branching ratios for the levels above the α-decay threshold. The present data provide new relevant information on the partial widths for several high lying states in ^{18}Ne which is used to calculate the ^{14}O$(\alpha,$p$)^{17}$F reaction rate.

II. EXPERIMENT

The experiment was carried out at the Nuclear Science Laboratory (NSL) at the University of Notre Dame. A 15 MeV ^{3}He pulsed beam with nanosecond-wide resolution and 200 nanosecond period was produced by the FN tandem accelerator at NSL and used to bombard a 100 μg/cm^2 thick self-supported SiO target. The schematic view

of the experimental setup is shown in Fig. 3. The reaction products were measured by an array of 16 liquid organic scintillation detectors which measured the neutrons from the reaction ^{16}O(^{3}He,n) and a Low Energy Silicon-strip detector Array (LESA) [12, 13] which was used to measure the charged particle decays from the resonance levels in ^{18}Ne. The neutron detector array was placed 3.6 meters away from the center of the reaction chamber covering an angular range from 11° to 39°. The beam stop was surrounded by tanks filled with borated water in order to shield neutrons generated at the beam stop from coming to the detectors. The array of neutron detectors consisted of four hexagonal 5″ thick detectors, five 7″×1″ cylindrical detectors, and seven 5″×2″ cylindrical detectors. The silicon detectors array LESA consisted of 4 identical 300 μm thick silicon-pad detectors, each of which has 4 strips and a total area of 4×4 cm^2. The silicon detector array was placed inside the reaction chamber, covering an angular range from 90° to 150°. The neutron detectors and the silicon detectors measured in coincidence mode the reaction products.

To subtract the contribution of silicon in the target and possibly carbon contamination, measurements with a pure Si target and a pure carbon foil were also done. The environmental background of the neutron Time-of-Flight spectra was obtained from long runs without beam on target. The silicon background was removed by subtracting Si runs from SiO runs matched at the peak produced by the ground state of ^{30}S. The silicon background subtraction is shown in Fig. 4. The energy levels in ^{18}Ne were identified in the neutron detector array using Pulse Shape Discrimination (PSD) and Time-of-Flight (ToF) methods [14]. The PSD technique was performed with four MPD4 Mesytec modules [15]. A typical 2-d plot for demonstrating the PSD is shown in Fig. 5. The energy of neutrons was obtained from ToF. It was therefore possible to identify from which energy level in ^{18}Ne the neutron group was coming. A typical neutron ToF spectrum after background subtraction with the identification of different levels in ^{18}Ne is shown in Fig. 6.

The various charged particle decays from the populated levels in ^{18}Ne were identified from their coincidences with neutrons. Levels above the proton threshold are expected to decay by charged particle emission and be detected in the silicon detectors. The particle identification was done on a "strip-by-strip" basis. A complete kinematics reconstruction was performed. For each energy level identified in the neutron detectors we calculated the kinematics for the possible open channels of charged particle decays that would be detected in each strip of the silicon detectors. We considered the open decay channels by proton emission to the ground state of ^{17}F, proton emission to the first excited state of ^{17}F at E$_x$ = 0.4953 MeV, two proton decay to the ground state of ^{16}O and α-decay to the ground state of ^{14}O. Proton decay to higher excited states in ^{17}F were not considered since the next level is at very high excitation energy with respect to the ground state (E$_x$ = 3.104 MeV). After the different decay channels were kinematically identified, an "event-by-event" reconstruction for each energy level was made with the specific kinematic shifts for a chosen channel (p, p', $2p$ and α) to add up all the sixteen strips of the silicon detectors. In the case of two proton decay, we considered only the di-proton system (^{2}He) in the kinematic reconstruction for simplicity.

III. RESULTS AND DISCUSSION

The reconstructed energy spectra of charged particles in coincidence with neutrons are shown in Fig. 7. For each level, kinematics used in the "event-by-event" reconstruction of different portions of the spectra is color coded.

The angular correlations of the decaying charged particles from the excited states in the parent compound nucleus ^{18}Ne can be analyzed using the formalism described by Noe *et al.* [16], where the full angular correlation can be obtained by fitting the experimental data in limited angular range. Unfortunately in the present case, the proton decay channel to the ground state of ^{17}F dominates over all the other channels such that poor statistics for the p'- and α- channels prevent such a fitting procedure. However, the angular dependence is weak for decay from a compound nucleus for light projectiles at low energies and it is mainly related to the angular momentum transfer in the entrance channel [17]. The large coverage of LESA for the detection of charged particles (11° - 39°) further reduces the significance of the angular dependence on the determination of decay branching ratios. Nonetheless, the angular distributions of the proton decay channel from the excited states in ^{18}Ne to the ground state of ^{17}F were extracted from the data and fitted with a linear combination of Legendre polynomials of the type: $a_0P_0 + a_2P_2 + a_4P_4 + a_6P_6$, where P_k are the Lengedre polynomials of order k. The angular distributions and their corresponding fittings are shown in Fig. 8. The fit function was integrated and compared with a flat curve resulting from assuming isotropic distribution in the angular range of 90° to 150°. The difference of the ratio of the two integrals from one provides an estimate of the error for omitting the angular dependence of the distributions. The coefficients of the fitting of the angular distributions and the ratio of the integrals are shown in Table I. The integrals of the fitted distributions from different levels are all within 10 % of the corresponding isotropic ones. For the branching ratio calculations, the ratio is taken for the same level which reduces the error even more. In order to extract the decay branching ratios, we assumed that the coverage of LESA for different decay mechanisms is the same. For a similar reaction system and setup [13], the isotropic distribution assumption was a reasonable estimate up to a 5 % error.

The resulting branching ratios for the ^{18}Ne energy levels at E_x = 5.10 MeV, E_x = 6.15 MeV, E_x = 6.30 MeV, E_x = 7.06 MeV, E_x = 7.95 MeV and E_x = 8.09 MeV, are shown in Fig. 7. The additional peaks on the right of the main proton decay peak are contaminations from the neighboring levels. Note that α-decays, in particular from the 7.95 and 8.09 MeV states, are observed for the first time in this work.

A summary of the results extracted from this experiment is shown in Table II.

A. The ^{18}Ne level structure

We measured the properties of six states in ^{18}Ne at excitation energies E_x = 5.10 MeV, E_x = 6.15 MeV, E_x = 6.30 MeV, E_x = 7.06 MeV, E_x = 7.95 MeV and E_x = 8.09 MeV. All these states have been reported before. In the following, we discuss our results in the context of previous measurements.

1. E_x = 5.10 MeV

There are two states at E_x = 5.09 MeV and E_x = 5.15 MeV which we do not have the resolution to separate. The one at E_x = 5.09 MeV is just below the α-decay threshold while the other at E_x = 5.15 MeV is slightly above the threshold. Wiescher *et al.* [1] identified those states as the mirror levels of E_x = 5.09 MeV and E_x = 5.26 MeV in ^{18}O. According to this consideration it was assigned $J^\pi = 3^-$ and 2^+ respectively without ruling out a swap in the spin-parity assignments. Nero *et al.* [20] measured $\Gamma = 40\pm20$ keV for E_x = 5.09 MeV level and $\Gamma = 25\pm15$ keV for E_x = 5.15 MeV for this doublet. Hahn *et al.* [2] measured $\Gamma = 45\pm5$ keV and assigned $J^\pi = 2^+$ for the level at E_x = 5.11 and $\Gamma \leq 15$ keV with $J^\pi = 3^-$ for the one at E_x = 5.15 MeV based of the analysis of transfer reactions. Gomez del Campo *et al.* [11] reported $\Gamma = 45\pm2$ keV for the level at E_x = 5.05 MeV and assigned $J^\pi = 2^+$ based on R-matrix analysis. Our results give a state at E_x = 5.10$\pm$0.10 MeV with contribution from the p- and p'-channels with the ratio $\frac{\Gamma_{p'}}{\Gamma_p} = 0.124$ that has been measured for the first time.

2. E_x = 6.15 MeV

Much effort has been spent on studying the properties of the E_x = 6.15 MeV level. This is by far the most significant level for the ^{14}O(α,p) reaction rate. Wiescher *et al.* [1] predicted this $J^\pi = 1^-$ level at E_x = 6.125 MeV with $\Gamma = \Gamma_p$ = 51 keV from the mirror state in ^{18}O. Hahn *et al.* [2] also identified this level as $J^\pi = 1^-$ and $\Gamma \leq 40$ keV based on the analysis of transfer reactions. Blackmon *et al.* [7] relied on R-matrix fits to assign $J^\pi = 1^-$ with $\Gamma = 58\pm2$ keV, $\Gamma_\alpha = 8\pm2$ eV and $\frac{\Gamma_{p'}}{\Gamma_p} = 2.4$. Note that they reported an unusually large p' branching. A similar measurement was done by He *et al.* [8] reporting also a strong inelastic p' branching but not to the degree suggested in reference [7] with $\frac{\Gamma_{p'}}{\Gamma_p} \sim 1$. The FSU group based on their work using the ANC method to study the mirror level in ^{18}O, suggested a value of $\Gamma_\alpha \approx 2$ eV [10]. Gomez del Campo *et al.* [11] reported observation of two-proton decay from this level with 18 eV $\leq \Gamma_{2p} \leq$ 63 eV, assigning $J^\pi = 1^-$ with $\Gamma = 50\pm5$ keV.

Our results give a state at E_x = 6.15$\pm$0.08 MeV. The main decay channel measured for this state is by p-decay to the ground state of ^{17}F. This energy level is much less populated than the neighboring level at E_x = 6.30 MeV which contaminates the corresponding reconstructed spectrum shown in Fig. 7.

While the aim of this work was the measurement of branching ratios and not the search for two-proton decay, this channel is in fact open for the energy levels considered in the ^{14}O(α,p)^{17}F reaction rate. This decay channel was explored on the basis of kinematics (considering only the di-proton system (^{2}He) in the kinematics reconstruction for simplicity). Only the level at E_x = 6.15 MeV showed some evidence of this exotic type of decay. There is an excess of counts in the energy region corresponding to *2p*-decay channel that may suggest its existence. While this is not direct evidence of *2p*-decay since we did not detect the two individual protons, an excess of counts was estimated for this resonance by taking the background level from the energy region corresponding to *2p*-decay in the neighboring level at E_x = 6.30 MeV where there is no evidence of this type of decay, and scaling it by the ratio of the corresponding areas of peaks in the neutron ToF spectra. Similar estimate was done also for the p' channel.

Due to large uncertainties, only the upper limits of the branching ratios for the *p'*- and *2p*-channels were estimated at a 95 % confidence level using Bayesian approach [19] assuming that the net excess of counts were from real decay events. These branching ratios are given in Table II. There is a strong discrepancy in these partial decay branchings between our results and the previously reported values [7, 8, 11]. The strong p' branchings previously reported for this level by [7, 8] are excluded by the upper limit of the present work. The upper limit of the branching ratio corresponding to the *2p*-decay channel is at least two orders of magnitude bigger than previous estimates [11, 18].

In order to prove or to definitely rule out the *2p*-decay, further experiments are needed where the two protons can be directly measured. It is important to point out that the results obtained in this work are extracted by directly counting and comparing the areas corresponding to the different decay channels.

Branching ratios of this work, the total width from Gomez del Campo *et al.* [11], and the α width from the FSU estimate [10] for this level are adopted in the rate calculation. We have calculated the impact on the reaction rate of interest by assuming both, with and without *2p* branching for this resonance.

3. $E_x = 6.30$ MeV

There is a doublet state at $E_x = 6.3$ MeV. Wiescher *et al.* [1] predicted a $J^\pi = 4^+$ state at $E_x = 6.30$ MeV and a $J^\pi = 3^-$ one at $E_x = 6.35$ MeV. Hahn *et al.* [2] suggested a state at $E_x = 6.286$ MeV with $J^\pi = 3^-$, $\Gamma_\alpha = 0.34$ eV and $\Gamma \leq 20$ keV; and a $J^\pi = 2^-$ at $E_x = 6.345$ MeV with $\Gamma = 45\pm10$ keV. Gomez del Campo *et al.* [11] observed a state with $J^\pi = 2^-$ at $E_x = 6.35$ MeV with $\Gamma \sim 50$ keV. Park *et al.* [21] measured $\Gamma = 8\pm7$ keV for the state at $E_x = 6.305\pm.004$ MeV. In the present work, we measured a state at $E_x = 6.30\pm0.05$ MeV with nearly 100 % proton decay to the ground state of ^{17}F. For the reaction rate calculation, the unnatural-parity 2^- level at $E_x = 6.35$ MeV is not considered since it does not contribute to the rate.

4. $E_x = 7.06$ MeV

For this broad state at $E_x = 7.06$ MeV, Wiescher *et al.* [1] had adopted a $J^\pi = 1^-$ and $\Gamma = 180\pm50$ keV. Funck and Langanke [22] identified this state as $J^\pi = 4^+$ as member of the $\alpha + {}^{14}$O molecular band. The analysis of Hahn *et al.* [2] also leads to $J^\pi = 4^+$ as well as that of Harss *et al.* [6] who also gave $\Gamma = 90\pm40$ keV, $\Gamma_\alpha = 40\pm14$ eV and $\Gamma_{p'} \leq 1$ keV. From the analysis of the direct measurement performed by Notani *et al.*, it was reported a strong proton decay from this state to the first excited state of ^{17}F "that would suggest an increase of 50 % for the ^{14}O(α,p)^{17}F reaction rate" [9]. Our results gave a state at $E_x = 7.06\pm0.04$ MeV with the ratios $\frac{\Gamma_{p'}}{\Gamma_p} = 0.19$ and $\frac{\Gamma_\alpha}{\Gamma_p} \leq 0.01$. The small p' branching reported in this work suggests that the p' channel from this level does not contribute to the rate to the extent indicated by Notani *et al.*

5. $E_x = 7.95$ MeV

Wiescher *et al.* [1] adopted a state at $E_x = 7.915$ MeV as $J^\pi = 1^-$. Hahn *et al.* [2] reported this level at $E_x = 7.92\pm0.02$ MeV with $\Gamma = 70\pm20$ keV via the ^{20}Ne(p,t) reaction and at $E_x = 7.94\pm0.01$ MeV with $\Gamma = 40\pm10$ keV via the ^{16}O(^{3}He,n) reaction. We adopted the average of their total width results $\Gamma = 55\pm20$ keV for calculating the rate. We measured a state at $E_x = 7.95\pm0.03$ MeV, with branching ratio of $\frac{\Gamma_{p'}}{\Gamma_p} = 0.25$ and $\frac{\Gamma_\alpha}{\Gamma_p} = 0.31$. Note that a significant α branching is observed for the first time. In absence of experimental information we chose the average of the possible spin values, $J^\pi = 3^-$ for the rate calculation.

6. $E_x = 8.09$ MeV

Wiescher *et al.* [1] assigned $J^\pi = 5^-$ to this level on the basis of mirror states in ^{18}O. Hahn *et al.* [2] observed such a level at $E_x = 8.11\pm0.10$ with $\Gamma \leq 30$ keV. We measured a level at $E_x = 8.09\pm.03$ MeV with branching ratio of $\frac{\Gamma_{p'}}{\Gamma_p} = 0.21$ and $\frac{\Gamma_\alpha}{\Gamma_p} = 0.32$. A significant α branching from this level is also observed for the first time. In absence of experimental information we chose the average of the possible spin values, $J^\pi = 3^-$ for the rate calculation.

B. Astrophysical implications

The resonance contribution of the ^{14}O(α,p)^{17}F reaction rate was calculated using the expression [23]

$$N_A < \sigma v >= 1.54 \times 10^{11} A^{-3/2} T_9^{-3/2}$$
$$\times \sum_i \omega\gamma_i \, exp\left(-\frac{11.605 E_i}{T_9}\right) \tag{1}$$

with A being the reduced mass (amu), E_i the resonance energy in the center of mass system (MeV), and T_9 is the temperature (10^9 K). The resonance strength $\omega\gamma$ in MeV is defined as

$$\omega\gamma = \frac{2J+1}{(2I_\alpha+1)(2I_T+1)} \times \frac{\Gamma_\alpha \Gamma_{p_{tot}}}{\Gamma} \qquad (2)$$

where J, $I_\alpha = 0$ and $I_T = 0$ are the total angular momentum of the resonance, the α-particle, and the ^{14}O, respectively. Γ_α is the α-width, while $\Gamma_{p_{tot}} = \Gamma_p + \Gamma_{p'}$ is the total proton-width and $\Gamma = \Gamma_{p_{tot}} + \Gamma_{2p} + \Gamma_\alpha$ is the total width of the state.

Due to the fact that in the entrance channel, both the ground states of ^{14}O and α are 0^+, the ^{14}O$(\alpha,$p$)^{17}$F reaction is expected to proceed only through natural parity states.

For simplicity of discussion and comparisons with previous studies, we did not include the contributions from direct reactions and their interference contributions to the reaction rate. The details and effects of these contributions were taken into account in the works by Wiescher $et\ al.$ [1] and Hahn $et\ al.$ [2].

We made use of all the experimental and theoretical information gathered for ^{18}Ne in order to calculate the resonance reaction rate. We present the calculation of the reaction rate using for the first time, all the new information extracted from the branching ratios of all five states (E$_x$ = 6.15 MeV, E$_x$ = 6.30 MeV, E$_x$ = 7.06 MeV, E$_x$ = 7.95 MeV and E$_x$ = 8.09 MeV) above the α-decay threshold of ^{18}Ne. We did not obtain information about the total widths of the levels since we did not have the resolution to measure most of them. For this reason, we took the total widths measured with better resolution from previous works and used our branching ratios to calculate the partial widths. It is important to point out that the ratio of the partial widths $\Gamma_{p'}/\Gamma_p$ is very important to the determination of the reaction rate from the measurement of the inverse reaction ^{17}F(p,$\alpha)^{14}$O and to resolving the discrepancies between previous studies [6–8].

The new resonance parameters used in the calculation of the ^{14}O$(\alpha,$p$)^{17}$F resonance reaction rate are shown in Table III. There are several states that we did not observe in the present work but have been suggested in previous studies. Some of them are most probably unnatural parity and hence do not contribute to the reaction rate. For the sake of completeness, we also considered the resonance contributions from the possible natural-parity levels at E$_x$ = 5.15 MeV, E$_x$ = 7.37 MeV and E$_x$ = 7.60 MeV that were not observed in the present work but seen previously [2, 6]. Properties of these levels are listed in the last three rows of Table III.

Fig. 9 shows the resonance contributions from individual levels to the ^{14}O$(\alpha,$p$)^{17}$F reaction rate using the set of parameters given in Table III. The resonance contribution of the most important 6.15 MeV state dominates the rate in the temperature range $0.1 \leq T_9 \leq 1.5$. As a result, the reaction rate depends almost entirely on this specific resonance. At higher temperatures (T$_9 \geq 1.5$), the higher energy resonances start to play an important role (contributing > 20 % to the rate) and eventually dominate the ^{14}O$(\alpha,$p$)^{17}$F reaction rate at temperatures T$_9 \geq 2$. Three previously reported resonances at E$_x$ = 5.15 MeV, E$_x$ = 7.37 MeV and E$_x$ = 7.60 MeV that were not observed in the present work are also included for comparison here. The resonance at E$_x$ = 5.15 MeV is basically negligible because it is too close to the α-decay threshold. The possible resonances at E$_x$ = 7.37 MeV and E$_x$ = 7.60 MeV [6] may have small contributions to the resonance reaction rate at high temperatures but not as significant as the other observed resonances.

The effects of the extra three resonances not measured in the present work but observed in previous ones are shown in Fig. 10 as ratios of the rates to that of Hahn $et\ al.$ [2].

The new ^{14}O$(\alpha,$p$)^{17}$F resonance rate calculated in the present work as well as the previous ones by Wiescher $et\ al.$ [1], Hahn $et\ al.$ [2], Harss $et\ al.$ [6], and Blackmon $et\ al.$ [7] are shown in Fig. 11 as ratios to the rate of Hahn $et\ al.$ [2]. Another rate with a 50 % increase from the p'-channel of the 7.06 MeV state suggested by the work of Notani $et\ al.$ [9] is not shown in the plot. Different values of α- and p-width parameters for the two most important states at 6.15 and 7.06 MeV used in these proposed reaction rates are listed in Table IV. The two dramatic enhancements in the rate proposed by Blackmon $et\ al.$ [7] and Notani $et\ al.$ [9] are essentially excluded by the upper limits of our new measurements of small p'-decay branching ratios for both the 6.15 and 7.06 MeV states.

The influence of the possible $2p$ is also shown in Fig. 11. A large $2p$-decay branching ratio would effectively reduce the total proton width and hence the resonance strength. Taking the upper limit of our measurement, the net effect would be to decrease the ^{14}O$(\alpha,$p$)^{17}$F reaction rate by a small amount represented by the shadowed area.

For the reaction rates of Hahn $et\ al.$ [2], Harss $et\ al.$, and this work in Fig. 11, the discrepancies at low temperatures (T$_9 \leq 1$) are largely determined by the α-width of the 6.15 MeV level. The discrepancies at high temperatures (T$_9 \geq 2$) are from the contributions of higher lying levels.

At typical Novae outburst peak temperatures ranging between $0.1 \leq T_9 \leq 0.4$ [24], the reaction rate is dominated by the 6.15 MeV level and its partial decay branching ratios. The main difference among the new rate calculated in this work and previous ones in this temperature range is due to the partial α-width. The reaction rate calculated using an eventually large $2p$-decay branching suggested in this work would effectively reduce the resonance strength. Whether the state has a two proton branch of the order observed by Gomez del Campo $et\ al.$ [11] or by the upper

limit indicated by the excess of counts suggested here with all the caveats, the effect on the resulting reaction rate is still small.

At typical X-ray bursts peak temperatures of 1-2 GK [25], higher energy resonances start to play more important roles in the rate. In particular, the large enhancement of the rate from the present work in comparison with the previous ones at $T_9 \geq 3$ shows the dominant contributions from the 7.95 and 8.09 MeV states measured in this work. These enhancement effects arise from the large α-branching measured for such resonances in the present work for the first time. The new rate based on the new experimental information resulting from this work provides more accurate input for model simulations of these explosive astrophysical events.

IV. CONCLUSIONS

We populated resonance states in ^{18}Ne using the ^{16}O(^{3}He,n) reaction. A coincidence measurement between neutrons and decaying charged particles shed light on the level structure of ^{18}Ne above the α-decay threshold. Our aim was to measure the branching ratios. We obtained new experimental information on the branching ratios for six ^{18}Ne states: $E_x = 5.10$ MeV, $E_x = 6.15$ MeV, $E_x = 6.30$ MeV, $E_x = 7.06$ MeV, $E_x = 7.95$ MeV and $E_x = 8.09$ MeV. We used the total widths from previous works and the new information on the branching ratios from this work to extract the partial widths. In particular, our results for the decay branchings of the 6.15 and 7.06 MeV levels are dramatically different from previous estimates. The contribution from the inelastic branch to the ^{14}O(α,p)^{17}F reaction rate was determined to be small. On the other hand, the strong contributions of the α-channels from the 7.95 and 8.09 MeV levels measured in this work can dramatically affect the rate at high temperatures.

In combination with previous results we provide a more accurate calculation of the ^{14}O(α,p)^{17}F resonance reaction rate. The reaction rate calculated with the new resonance parameters may facilitate further model studies of the Hot CNO cycle and its breakout paths in explosive astrophysical environments such as novae and X-ray bursts.

ACKNOWLEDGMENTS

[1] M. Wiescher et al., *Astrophys. J.* **316**, 162 (1987).
[2] K. I. Hahn et al., *Phys. Rev. C* **54(4)**, 1999 (1996).
[3] D. R. Tilley et al., *Nucl. Phys. A* **595**, 1 (1995).
[4] B. Harss et al., *Phys. Rev. Lett.* **82(20)**, 3964 (1999).
[5] J. C. Blackmon et al., *Nucl. Phys. A* **688**, 142 (2001).
[6] B. Harss et al., *Phys. Rev. C* **65**, 035803 (2002).
[7] J. C. Blackmon et al., *Nucl. Phys. A* **718**, 127 (2003).
[8] J. J. He et al., *Phys. Rev. C* **80**, 042801(R) (2009).
[9] M. Notani et al., *Nucl. Phys. A* **746**, 113 (2004).
[10] E. D. Johnson, G. V. Rogachev, J. Mitchell, L. Miller and K. W. Kemper, *Phys. Rev. C* **80**, 045805 (2009); G. V. Rogachev (Private communication).
[11] J. Gomez del Campo et al., *Phys. Rev. Lett.* **86(1)**, 43 (2001).
[12] W. P. Tan, J. L. Fisker, J. Görres, M. Couder and M. Wiescher, *Phys. Rev. Lett.* **98**, 242503 (2007).
[13] W. P. Tan et. al., *Phys. Rev. C* **79**, 055805 (2009).
[14] W. R. Leo, *Techniques for Nuclear and Particle Physics Experiments*, Springer-Verlag (1994).
[15] *MPD-4*, www.mesytec.com/datasheets/MPD-4.pdf.
[16] J. W. Noe et al., *Phys. Rev. C* **9**, 1 (1974).
[17] G. R. Satchler *Introduction to nuclear reactions*, Oxford University Press (1990).
[18] L. V. Grigorenko et al., *Phys. Rev. C* **65**, 044612 (2002).
[19] K. Nakamura et al., *J. Phys. G* **37**, 075021 (2010).
[20] A. V. Nero and E. G. Adelberger, *Phys. Rev. C* **24**, 1864 (1981).
[21] S. H. Park et al., *Phys. Rev. C* **59**, 1182 (1999).
[22] C. Funck and K. Langanke, *Nucl. Phys. A* **480**, 188 (1988).
[23] C.Iliadis, *Nuclear Physics of Stars*, WILEY-VCH (2007).

[24] J. José , M. Hernanz and C. Iliadis, *Nucl. Phys. A* **777**, 550 (2006).

[25] H. Schatz and K. E. Rehm, *Nucl. Phys. A* **777**, 601 (2006).

FIGURES

FIG. 1. (Color) Hot CNO cycles and their breakout paths towards the *rp-process*. In the present work we explore the $^{14}O(\alpha,p)^{17}F$ reaction along the path labeled as Breakout I.

FIG. 2. Energy levels of ^{18}Ne adapted from the compilation [3]. The levels that contribute to the $^{14}O(\alpha,p)^{17}F$ reaction are the natural-parity ones above the α-decay threshold ($E_x \geq 5.125$ MeV). For these energy levels, the p-, $p'-$, *2p*- and α-decay channels are open and may need to be considered in the calculation of the reaction rate.

FIG. 3. Schematic view of the experimental setup. The neutron detectors were placed 3.6 meters away from the center of the reaction chamber covering an angular range from $11°$ to $39°$. The silicon detectors were placed inside the reaction chamber covering an angular range from $90°$ to $150°$.

FIG. 4. Silicon background subtraction from SiO target. The silicon background was subtracted from SiO target by scaling the Si run, matching the peak produced by the ground state of ^{30}S.

FIG. 5. (Color online) Pulse Shape Discrimination in the neutron detectors was performed with MPD4 Mesytec modules [15], allowing for a good n/γ discrimination. In the plot, γ signals (left) and neutron signals (right) can be easily distinguished by their shape and arrival time.

FIG. 6. Neutron Time-of-Flight spectrum for neutron detector N2 placed at $14°$ with respect to the beam. The identification of the different levels of ^{18}Ne is shown.

FIG. 7. (Color) "Event by event" reconstructed spectra for the resonance energy levels observed in ^{18}Ne. The different colors in the spectra correspond to different kinematics used to reconstruct the different portions of it, according to their respective decay channels (*p, p', 2p and α*). The branching ratios for the different decay channels are also shown. A possible indication of a *2p*-decay coming from $E_x = 6.15$ MeV level is observed (see discussion in the text).

FIG. 8. (Color online) Angular distributions of protons decaying form excited states in ^{18}Ne to the ground state of ^{17}F and their corresponding fit functions using Legendre polynomials.

FIG. 9. (Color) Contribution of the different resonance states in ^{18}Ne to the $^{14}O(\alpha,p)^{17}F$ reaction rate in the temperature range of $0.1 \leq T_9 \leq 5$. The solid lines represent the resonances measured in this work. The dashed lines correspond to resonances reported elsewhere but not observed in this work.

FIG. 10. (Color online) Ratio of the resonance contributions to the $^{14}O(\alpha,p)^{17}F$ reaction rates calculated in the present work to the calculated by Hahn *et al.* [2]. The rate labeled as *This work + 3* corresponds to the rate calculated in the present work plus contributions from three more resonances not observed in the present experiment but reported before at $E_x = 5.15$ MeV, $E_x = 7.37$ MeV, and $E_x = 7.60$ MeV.

FIG. 11. (Color online) Ratio of the resonance contributions to the $^{14}O(\alpha,p)^{17}F$ reaction rates calculated in the present work and the previous reported ones (Wiescher *et al.* [1], Hahn *et al.* [2], Harss *et al.* [6] and Blackmon *et al.* [7]) to the calculated by Hahn *et al.* [2]. The effect of a possible large *2p* decay would decrease the reaction rate by a factor represented by the shadowed area.

TABLES

TABLE I. Fitting parameters associated to Legendre Polynomials used to fit the proton angular distributions.

^{18}**Ne**	a_0	a_2	a_4	a_6	**ratio** [a]
5.15	1506.90	-819.45	-547.42	-802.13	0.92
6.15	194.80	-43.05	-22.06	-94.73	0.99
6.30	532.94	-193.96	111.55	0	0.99
7.06	1554.26	-109.72	-1230.54	-589.35	0.91
7.95	1116.96	-18.68	-428.29	-495.91	0.95
8.09	642.28	-47.26	-276.58	-299.72	0.94

[a] ratio of the integral of the fitting function to a flat function corresponding to an isotropic distribution in the angular range of 90° to 150°.

TABLE II. Summary of results for the energy levels in ^{18}Ne obtained in this work. The excitation energies (E_x) and the branching ratios (BR) for the different decay channels (p, p' and α) are provided.

^{18}Ne E_x (MeV)	Branching Ratios
5.10±0.10	$BR_p = 0.89\pm0.03$
	$BR_{p'} = 0.11\pm0.04$
6.15±0.083	$BR_{p'} \leq 0.21$ [a]
	$BR_{2p} \leq 0.27$ [a]
6.30±0.047	$BR_p = 1.00\pm0.02$
7.06±0.039	$BR_p = 0.83\pm0.03$
	$BR_{p'} = 0.16\pm0.07$
	$BR_\alpha \leq 0.01$
7.95±0.030	$BR_p = 0.64\pm0.08$
	$BR_{p'} = 0.16\pm0.10$
	$BR_\alpha = 0.20\pm0.09$
8.09±0.028	$BR_p = 0.65\pm0.12$
	$BR_{p'} = 0.14\pm0.12$
	$BR_\alpha = 0.21\pm0.13$

[a] Upper limits estimated at 95 % confidence level using the Bayesian approach [19]

TABLE III. Resonance parameters adopted in the calculation of the ^{14}O(α,p)^{17}F reaction rate.

E_x (MeV) [a]	E_x (MeV)	E_{res} (MeV)	J^π	Γ_α (eV)	Γ_p(keV)	Γ_{ptot} (keV)	Γ (keV)	$\omega\gamma$ (MeV)
6.15	6.15±.08	1.025	1^-	2 [d]	39.5±7	50±5	50±5[c]	6.00×10^{-6}
					26±6[g]	36.5±7[g]	50±5[c]	4.38×10^{-6} [g]
6.297	6.30±.05	1.172	3^-	0.34 [b]	8±7	8±7	8±7 [e]	2.38×10^{-6}
7.059	7.06±.04	1.934	4^+	40±10 [f]	73±32	90±40	90±40 [f]	3.60×10^{-4}
7.950	7.95±.03	2.825	3^-	$11\pm6.6\times10^3$	35±15	44±16	55±20 [b]	6.16×10^{-3}
8.086	8.09±.03	2.961	3^-	$6.3\pm3.9\times10^3$	20±4	24±5	30 [b]	3.53×10^{-2}
5.146			3^-[b]					3.0×10^{-57} [b]
7.37[f]			2^+[f]					2.16×10^{-4} [f]
7.60[f]			1^-[f]					3.06×10^{-3} [f]

[a] From TUNL evaluation [3]
[b] From Hahn *et al.*[2]
[c] From Gomez del Campo *et al.*[11]
[d] From Rogachev [10]
[e] From Park *et al.*[21]

TABLE IV. Comparisons of α and p width parameters for the 6.15 and 7.06 MeV states proposed in previous studies and this work.

	6.15 MeV		7.06 MeV	
	Γ_α (eV)	$\Gamma_{p'}/\Gamma_p$	Γ_α (eV)	$\Gamma_{p'}/\Gamma_p$
Wiescher *et al.*[1]	0.394		213	
Hahn *et al.*[2]	2.2		48	
Harss *et al.*[6]	3.2		40±14	≤ 1/90
Blackmon *et al.*[7]	8±2	2.4		
Notani *et al.*[9]			large[a]	
He *et al.*[8]		≈ 1		
FSU [10]	2			
This Work	2 [b]	≤ 0.27	40 [c]	0.19

[a] Large enough to increase 50 % the reaction rate.
[b] Adopted from Rogachev [10].
[c] Adopted from Harss *et al.*[6].
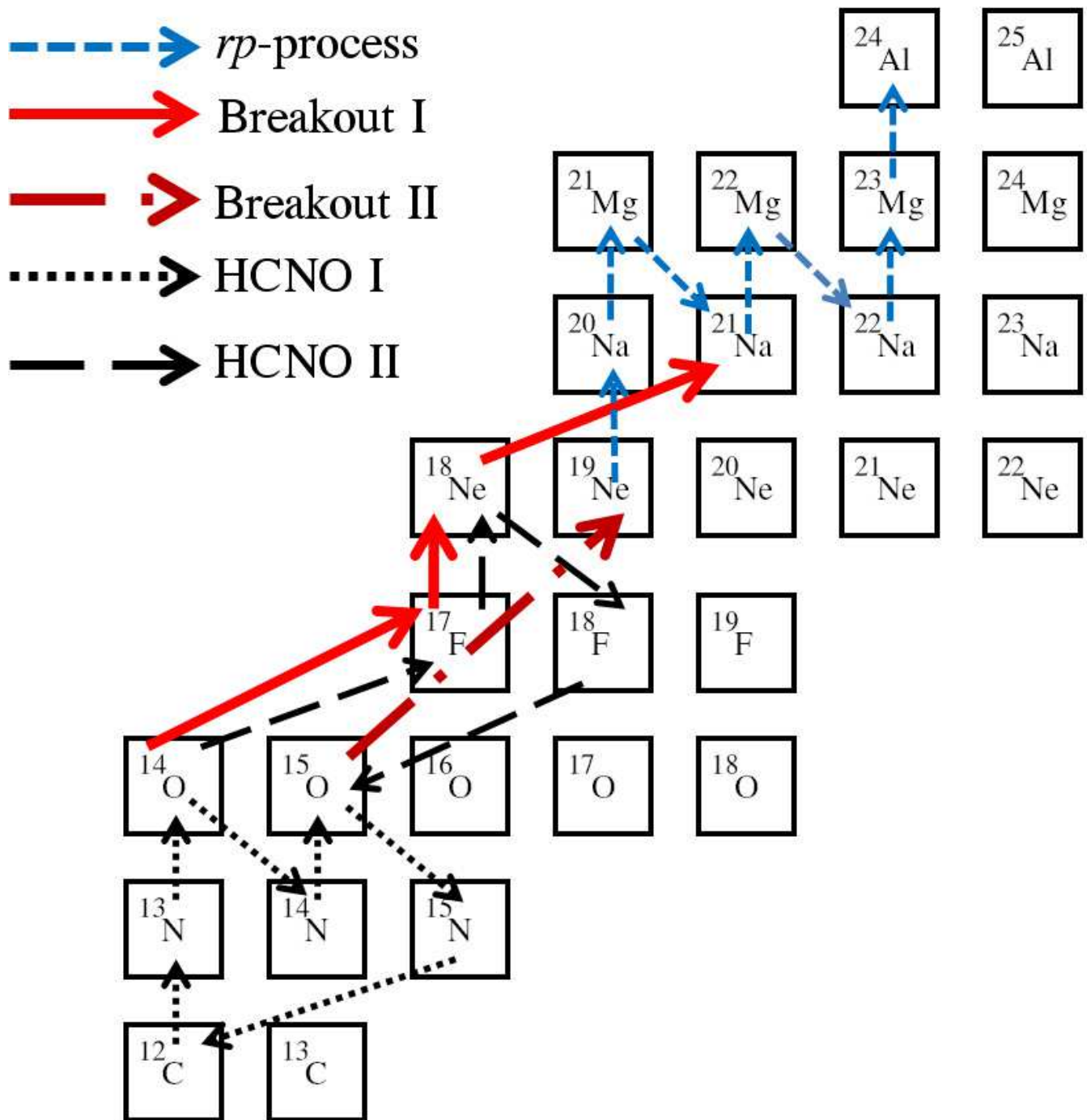
Figure 1   CJ10259   15May2012

9.20

8.50

8.09 7.91 7.95

7.71

7.35

7.06

6.15 6.30 6.35

5.45

5.09 5.15

5.125
$^{14}O+\alpha$

4.52 4.56 4.59   0⁺ 3⁺ 1⁻

4.429
$^{17}F+p'$

4.534
$^{16}O+2p$

3.934
$^{17}F+p$

3.6164 3.5763   0⁺ 2⁺
3.3762   4⁺

1.8873   2⁺

0⁺; T = 1

^{18}Ne
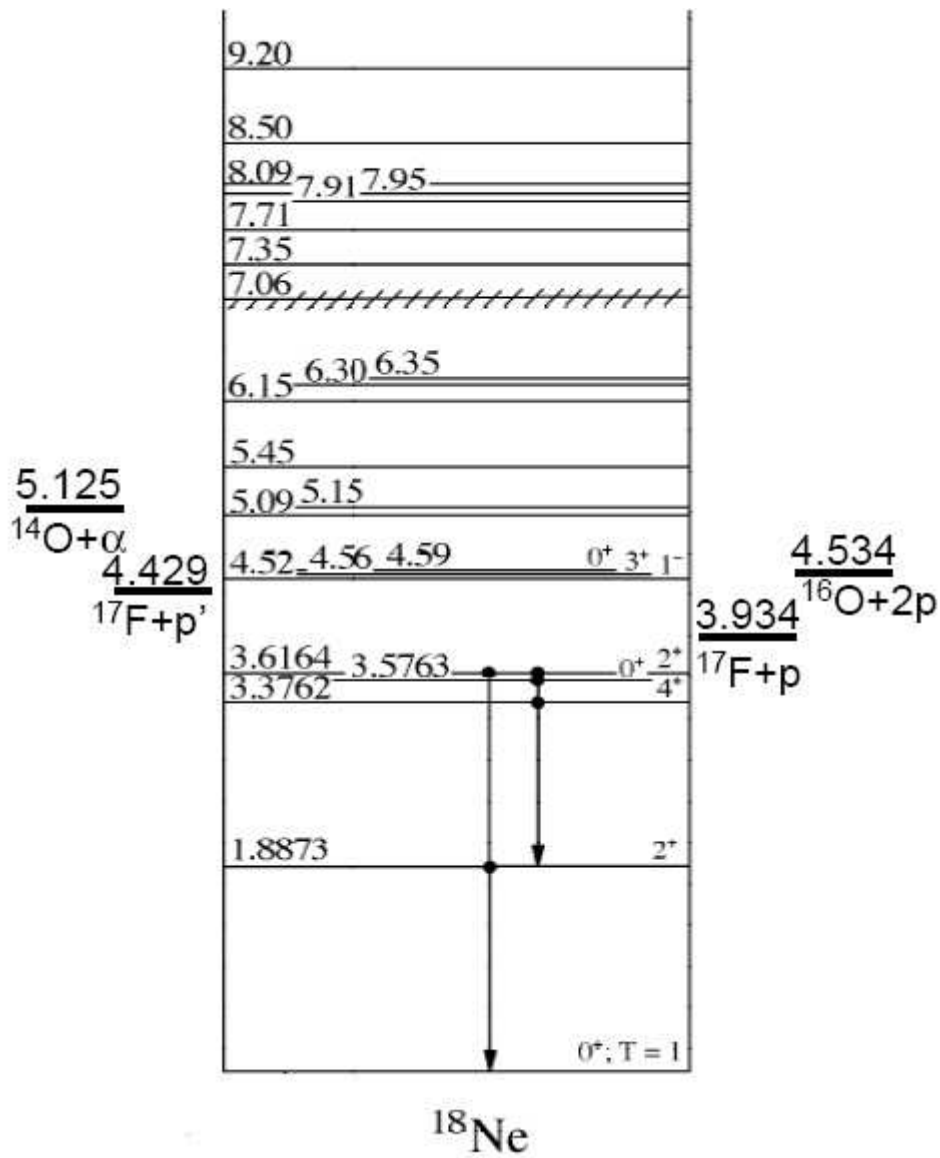
Figure 2   CJ10259   15May2012
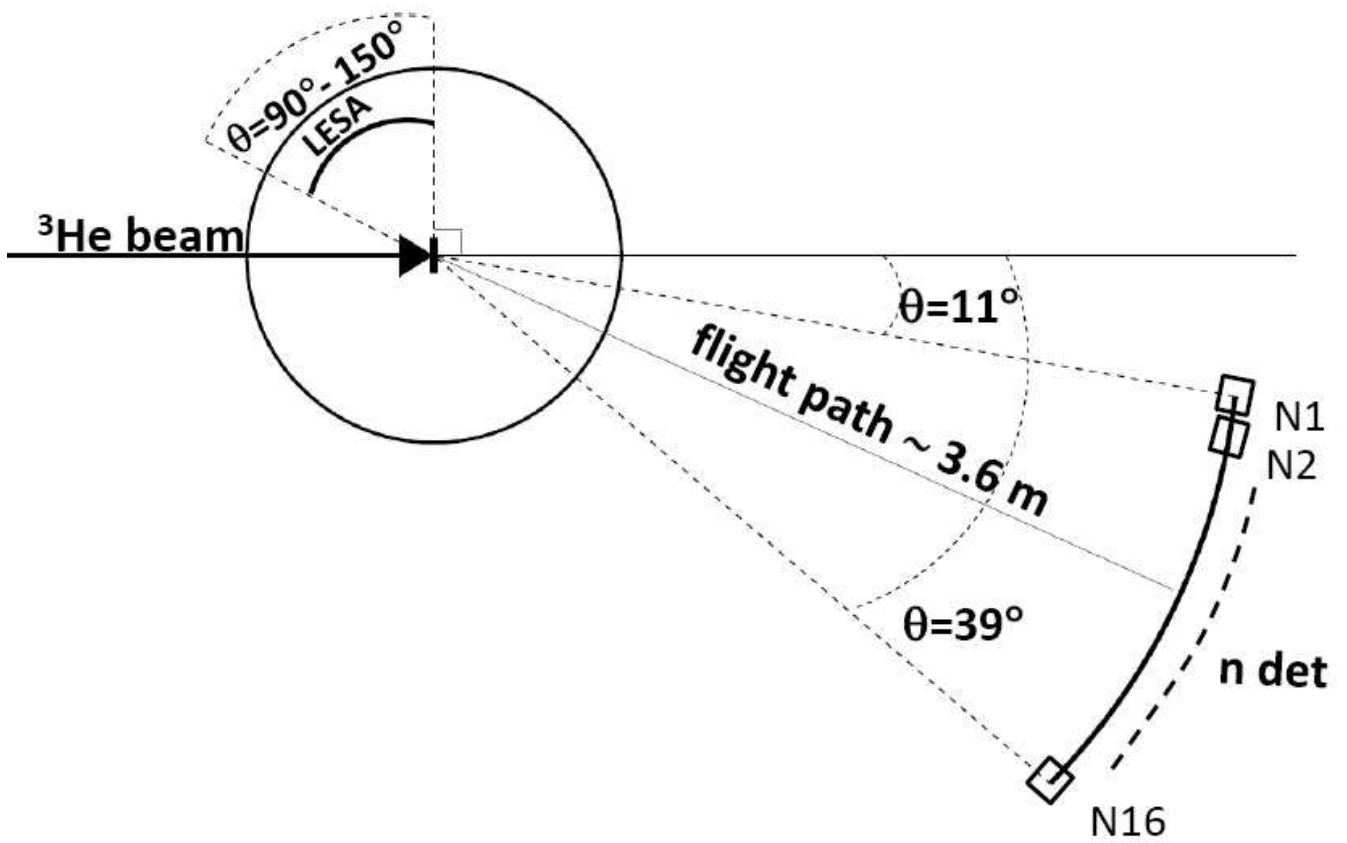
Figure 3   CJ10259   15May2012

Detector N2   14°

Counts

^{30}S g.s.

SiO target

Si target

ToF [ns/10]
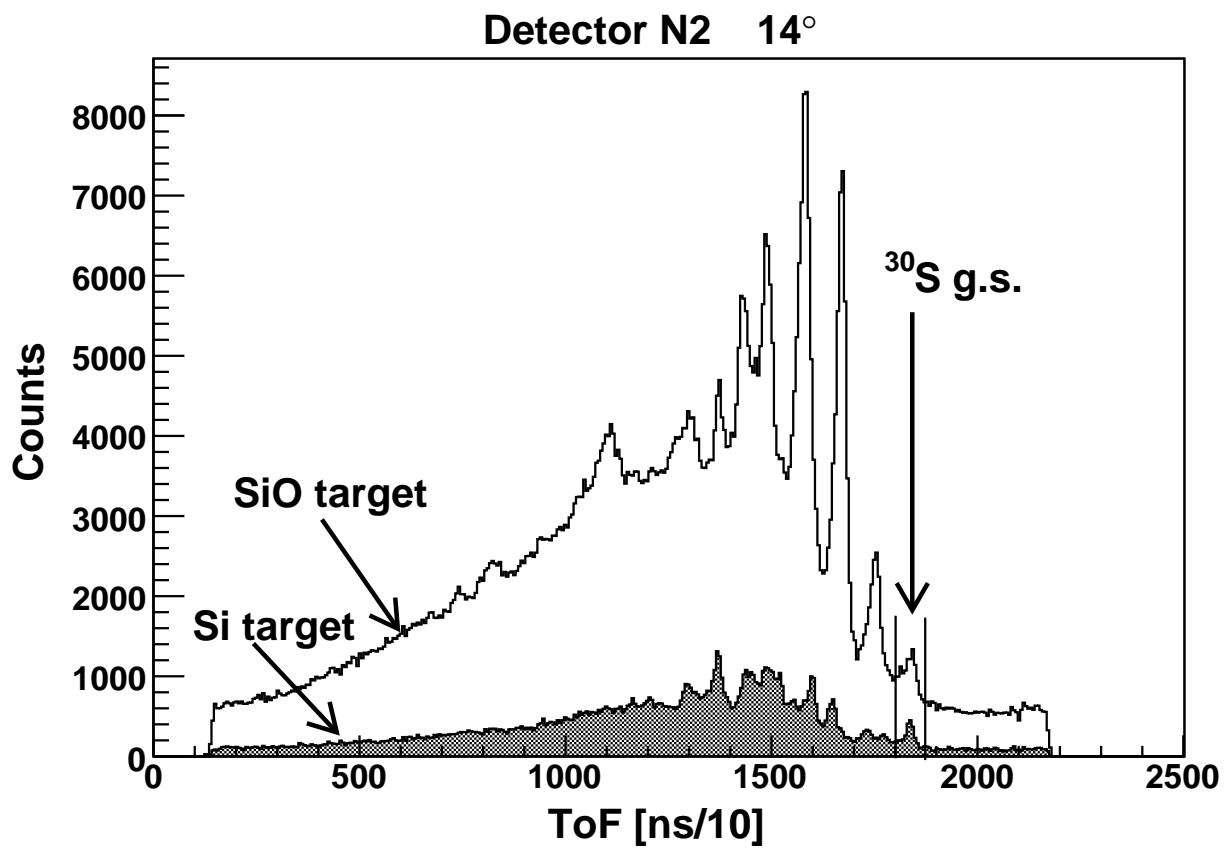
Figure 4   CJ10259   15May2012
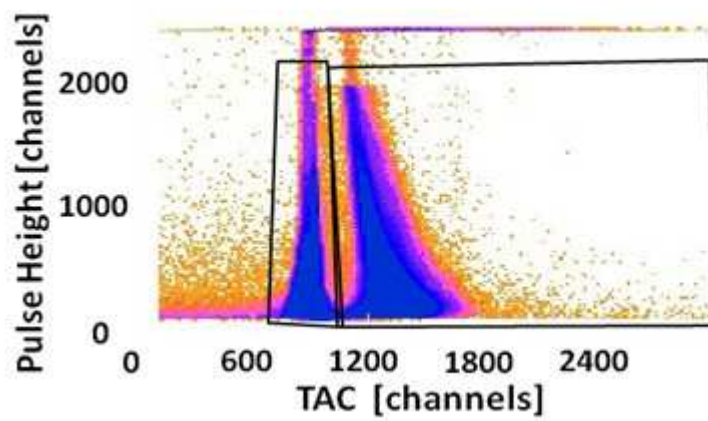
Figure 5   CJ10259   15May2012
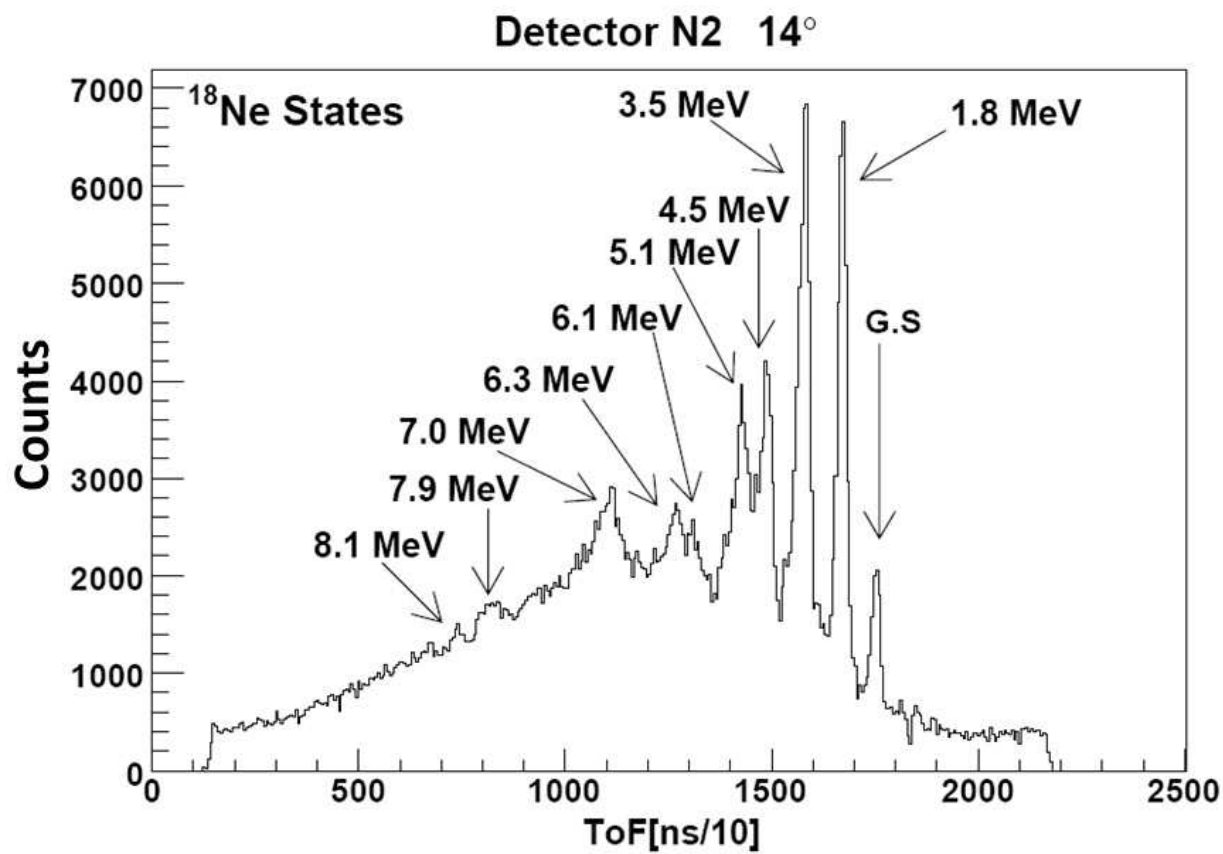
Figure 6   CJ10259   15May2012
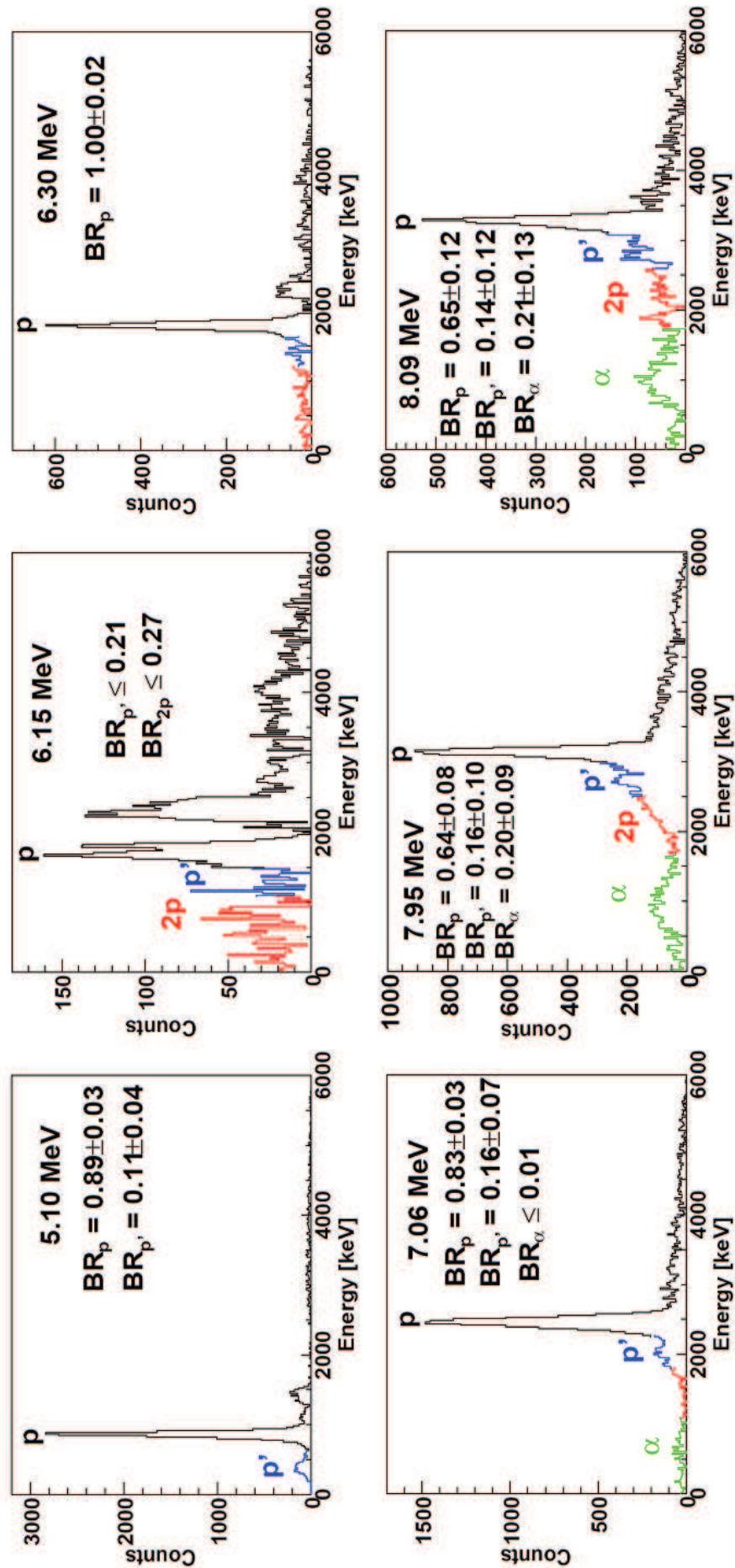
Figure 7   CJ10259   15May2012

|	5.15 MeV
	6.15 MeV
	6.30 MeV
	7.06 MeV
	7.95 MeV
	8.09 MeV
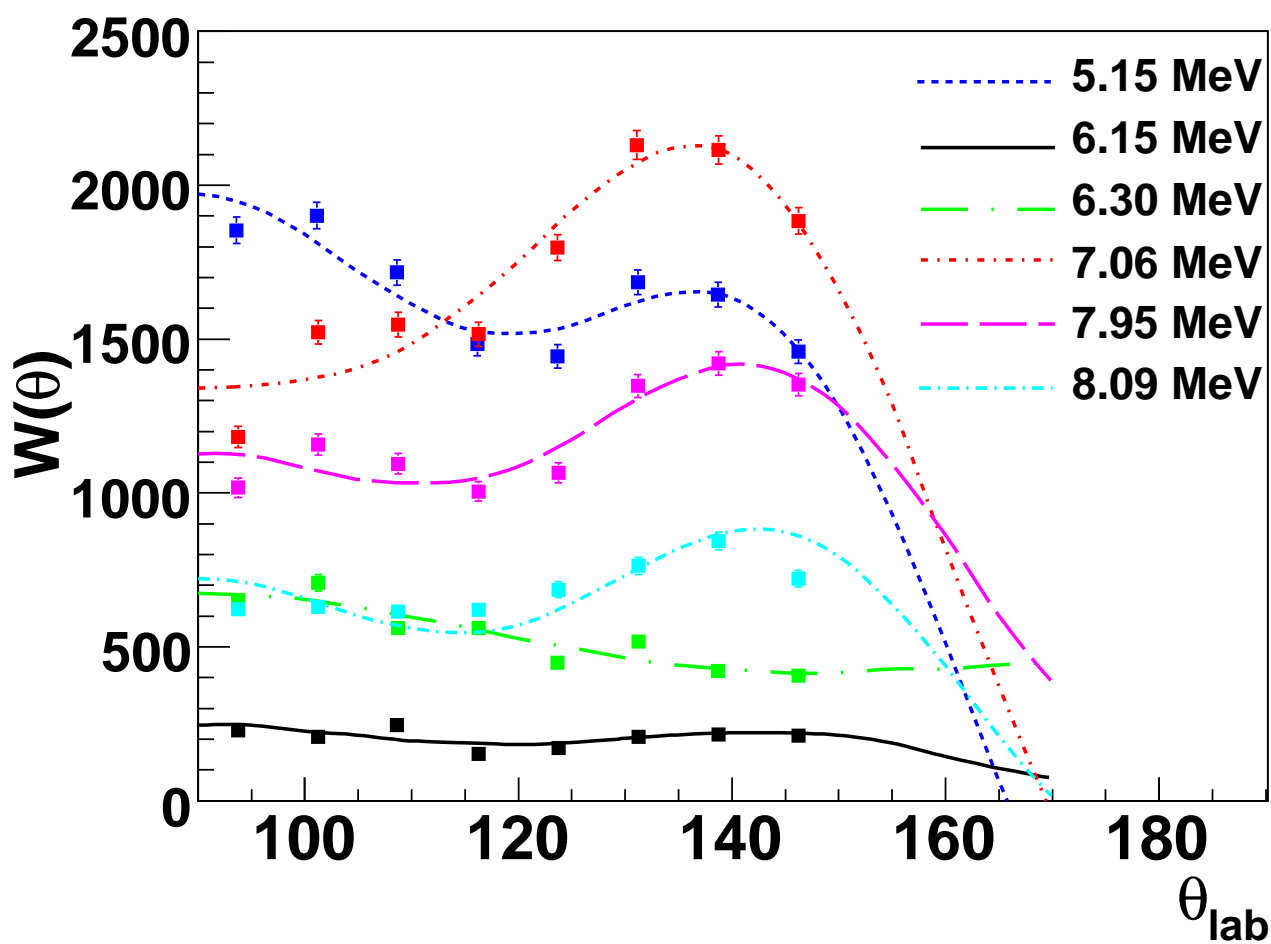
Figure 8   CJ10259   15May2012
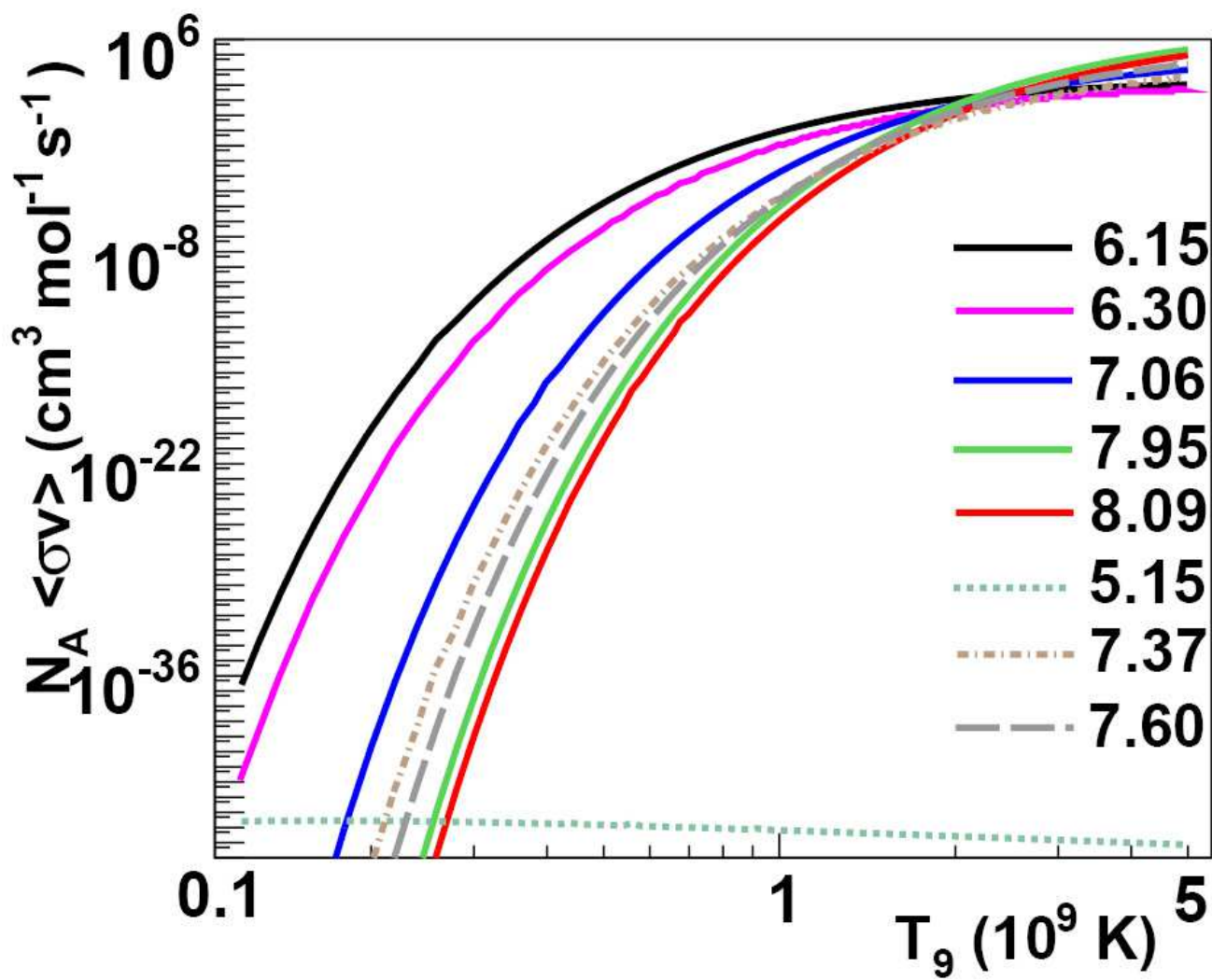
Figure 9   CJ10259   15May2012

Figure 10 CJ10259 15May2012

Figure 11   CJ10259   15May2012